

Adsorption of lanthanum(III), samarium(III), europium(III) and gadolinium(III) on raw and modified diatomaceous earth: equilibrium, kinetic and thermodynamic study

Imad Hamadneh^a, Noor W. Al-Jundub^a, Alaa A. Al-Bshaish^a, Ammar H. Al-Dujali^{b,*}

^aDepartment of Chemistry, Faculty of Science, University of Jordan, Amman 11942, Jordan, Tel. +962 786 341 111; email: imad72@hotmail.com (I. Hamadneh), Tel. +962 798 499 758; email: noorwajeh@yahoo.com (N.W. Al-Jundub), Tel. +962 789 637 017; email: alaastars55@yahoo.com (A.A. Al-Bshaish)

^bHamdi Mango Center for Scientific Research, University of Jordan, Amman, P.O. Box: 11942, Jordan, Tel. +962 796 629 774; email: ah.aldujaili@gmail.com

Received 9 May 2020; Accepted 5 November 2020

ABSTRACT

In the present work, naturally available diatomaceous earth (DE) was organically modified with hexadecyltrimethylammonium bromide (DE-HDTMA). The adsorption properties of DE and DE-HDTMA for lanthanum (La), samarium (Sm), europium (Eu) and gadolinium (Gd) ions in solution were studied. The effects of adsorbent dosages, ionic strength, and initial concentration of metal ions, adsorption time, pH value of solution and temperature on adsorption capacity were investigated. The results showed that the adsorption isotherms of DE and DE-HDTMA for metal ions satisfied the Langmuir, Freundlich and Dubinin–Radushkevich isotherms. By fitting the Langmuir equation, the saturated adsorption capacity of DE and DE-HDTMA for La(III), Sm(III), Eu(III) and Gd(III) ions can reach 185.185, 232.558, 117.647, 199.60, 111.048, 172.414, 92.593 and 156.250 mg g⁻¹, respectively. The mean free energy (E_{DR}) for adsorption of metal ions by DE and DE-HDTMA has been calculated from the Dubinin–Radushkevich equation and showed that the physisorption mechanism was operative. The adsorption kinetics confirmed to the pseudo-second-order kinetic equation. The calculated thermodynamic parameters revealed that the adsorption is a spontaneous and exothermic process.

Keywords: Lanthanides; Diatomaceous earth, Isotherm Adsorption; Kinetic; Hexadecyltrimethylammonium bromide

1. Introduction

The rare earth elements (REEs) are widely used in many technological devices, such as superconductors, magnets, catalysts, and batteries [1]. With the increasing use of REEs and inappropriate production and post-production treatments, the contaminations, which are related to the REEs, have emerged in recent years and are causing a series of environmental problems. The toxicity of REEs to humans is similar to those of lead, cadmium and other heavy

metals [2]. These hazards associated with REEs have highlighted the importance of extraction, recycling and removal of REEs from contaminated waters [3].

A number of technologies have been used for the separation and pre-concentration of REEs, such as co-precipitation [4], ion-exchange [5], and solvent extraction [6]. However, most of them have disadvantages such as secondary pollution, inefficiency, and high operational cost [7]. Therefore, the adsorption technique is considered to be

* Corresponding author.

the most efficient removal method due to its simplicity, low-cost, quick and lack of harmful by-products [8,9].

La(III), Sm(III), Eu(III) and Gd(III) ions have been used as homologs of trivalent actinide elements, due to their similar physicochemical properties. These four elements are a part of REEs family under category namely the light rare earth. Significant amounts of these four lanthanides exist in ores and polluted the environment, which needs separation and extraction. There are various adsorbent materials (raw and modified) used for the removal of REEs from aqueous solutions. There is a very good review article published in 2016, summarizing and discussing the published literature on the use of different adsorbents for REEs adsorption [10]. Thus, only the literature for the last three years concerning the adsorption of La(III), Sm(III), Eu(III) and Gd(III) ions are considered in this work. For example, the nanocomposite of graphite and magnetite [11] has been reported as a good adsorbent for adsorbing La^{3+} and Eu^{3+} from an aqueous solution. It was found that the adsorption process was very sensitive to solution pH, evidencing that electrostatic interactions are the main binding mechanism involved. Removal efficiencies up to 80% were achieved at pH 8, using only 50 mg L⁻¹ of the nanocomposite. Awual et al. [12,13] study to develop a highly selective Lewis base adsorbent to investigate the selective sorption and recovery of Eu(III) and Sm(III) from wastewater. They found that maximum adsorption capacities were 125.63 and 124.38 mg g⁻¹ for Eu(III) and Sm(III), respectively. Several natural clay minerals were used for the removal of La^{3+} [14]. The results illustrated that the structure and surface properties of natural clay minerals are the key factors that affect the La^{3+} adsorption, thus identifying the types of natural clay minerals and associated impurities in clay materials are important. The removal of La^{3+} and Sm^{3+} by amidoxime-hydroxamic acid polymer was investigated by Alakhras [15]. The adsorption of ions followed the following order: $\text{Sm}^{3+} > \text{La}^{3+}$ and follow the chemisorptions kinetic rate-determining step. The kinetic models for the adsorption of La^{3+} ions on poly-*o*-toluidine tungstophosphate were investigated by Khalil et al. [16]. It was found that both the pseudo-second-order and the homogeneous particle diffusion models were best to correlate the experimental rate data. Kusriani et al. [17] and Oyewo et al. [18] were used banana peel activated carbon as an adsorbent for the removal of La^{3+} and Sm^{3+} ions from an aqueous solution. The optimum condition for the adsorption of those two ions was determined to be a contact time of 2.5 h, a pH of 4, and an adsorbent dosage of 100 mg. Synthetic basaluminite was used for the removal of La^{3+} and the adsorption has been investigated with variable sulfate concentrations [19]. Experimental results show that adsorption onto basaluminite is strongly dependent on pH, starting at pH 5 for La^{3+} . Adsorption of Gd^{3+} from aqueous and nitric acid solutions using mesoporous potassium zinc hexacyanoferrate as nano ion exchanger material was investigated. Isotherm adsorption data were well fitted by the Freundlich and Dubinin-Radushkevich (D-R) adsorption isotherms model equation with a maximum adsorption capacity of 0.55 mg g⁻¹ at a pH of 4.5 and temperature of 25°C. Kinetic adsorption data were well fit with the pseudo-second-order equation [20]. The study carried out by Mohamed et al. [21] for the adsorption capacity of impregnation of trihexyl(tetradecyl)phosphonium bis(2,4,4-trimethylpentyl)phosphinate, as an

ionic liquid, into silica for removal of Gd^{3+} ions from aqueous solution. The experimental outcome revealed that the impregnation process enhanced the sorption behavior of silica, from 20% to 89.45% for Gd^{3+} ion. From the kinetic studies, the adsorption could be described well by the pseudo-second-order model; the results indicated that the Freundlich isotherm surpasses the Langmuir isotherm model for the adsorption process.

Diatomaceous earth and modified organically has been identified as a promising material for the environmental processes because it has a high affinity for the adsorption of many polluting agents of nuclear and environmental interest [22]. Its characteristics have been well documented, and their mechanisms of retention depend upon the metal chemical species [23]. Previously we have reported the use of the raw and organomodified diatomaceous earth (DE) as an adsorbent for organic and inorganic pollutants [24–28].

In continuation, we present here the adsorption of La(III), Sm(III), Eu(III) and Gd(III) ions from aqueous solutions using DE and DE-HDTMA – hexadecyltrimethylammonium bromide). The effect of various parameters including the initial concentration of metal ions, adsorbent dosage, pH, ionic strength, time and temperature on adsorption of these metal ions was investigated by batch techniques. The equilibrium and kinetic adsorption data were analyzed by Langmuir, Freundlich and D-R isotherm models and pseudo-first and pseudo-second-order kinetic models.

2. Experimental

2.1. Materials and equipment

Diatomaceous earth (DE) was obtained from the Natural Resources Authority (NRA), Amman, Jordan from the northeast of the capital Amman (Azraq Region). Lanthanum(III) acetate hydrate, samarium(III) acetate hydrate, europium(III) acetate hydrate, and gadolinium(III) acetate hydrate, arsenazo III indicator and hexadecyltrimethylammonium bromide (HDTMABr) were purchased from Sigma-Aldrich (Saint Louis, MO, USA 63178) with a grade higher than 99% and used without further purification.

Weighing samples was carried out using Precisa 410AM-FR (CH-8953 Dietikon, Switzerland) analytical balance. The pH of the solutions was measured with a HI9025 pH-meter. Fourier-transform infrared (FTIR) spectrum was recorded using Thermo Nicolet Nexus 670 FTIR spectrophotometer (Waltham, MA USA 02451). X-ray diffraction (XRD) and X-ray fluorescence (XRF) were recorded using Philips X'Pert PW 3060 (Eindhoven, Netherlands), operated at 45 kV and 40 mA. The shape and surface morphology of the samples were examined with the FEI inspect F50 (Tulsa, OK 74145) scanning electron microscopy (SEM). Shaking samples was carried out using the Köttermann 3047 shaker equipped with a thermostat. The concentrations of the metal ions were determined using UV-Vis Varian Cary 100 spectrophotometer. The specific surface area of the DE and DE-HDTMA and the cation exchange capacity (CEC) of DE were obtained using the procedure described in our previous publication [27]. The Brunauer-Emmett-Teller (BET) area and pore structure of the samples were obtained with a NOVA 2200e surface area and pore size analyzer

(Quantachrome Corp., Boynton Beach, FL, USA), from analyses of nitrogen gas adsorption isotherms at 77 K.

2.2. Preparation of stock solutions

Stock solutions of 1,000 mg L⁻¹ for the four metal ions were prepared separately by dissolving a specific amount of each metal salt of La(III), Sm(III), Eu(III) and Gd(III) in 0.01 M NaCl. The stock solutions were used to prepare solutions with different concentrations (5, 10, 15, 20, 25, 30, 35, 40, 45, and 50 mg L⁻¹), the dilution is achieved by using 0.01 M NaCl solution (to keep the ionic strength constant for all the different concentrations prepared). The pH of the solution was adjusted with 0.1 M HCl and 0.1 M NaOH solutions.

2.3. Preparation of DE and DE-HDTMA

The crushed and milled DE sample was washed several times with distilled water then dried in a drying oven to constant weight at 110°C. The samples were sieved, and fractions of 200 meshes and below were collected and stored in bottles. DE-HDTMA was prepared by the ion-exchange reaction. The amount of HDTMABr (8.5 g) equal to the CEC of DE (78 meq/100 g) was dissolved in 1 L distilled water and 30 g of diatomaceous earth was added and stirred with a mechanical stirrer for 24 h at 350 rpm. The DE-HDTMA clay was separated from the mixture by filtration, washed about five times with distilled water, and dried at 110°C for 3 h until constant mass.

2.4. Adsorption experiments

0.20 g of DE or DE-HDTMA adsorbent was placed in a solution containing one metal ion (concentration 5–50 mg L⁻¹) for adsorption at pH ranging from 1 to 7. All the adsorption experiments were carried out in a thermostatic water bath and the stirring speed was 150 rpm at a constant temperature of 25°C for 24 h. The adsorbed mixture was separated by centrifugation for 5 min at 2,500 rpm and filtered through a 0.45-micron filter, and the filtrates were collected to measure the final ion concentration using arsenazo III as an indicator. 4.0 mL of the prepared aqueous test solution from La(III), Sm(III), Eu(III) and Gd(III) ions at specific concentrations was added to a 50 mL volumetric flask, then 2.0 mL of 0.10 M HCl solution were added, then 1.0 mL of arsenazo III was transferred and dilution was done to the mark with 0.01 M NaCl solution [28]. The spectrophotometric determination was carried out within 30 min of sample preparation at 651 nm wavelength for Nd(III) and 653 nm wavelength for each Sm(III), Gd(III) and Eu(III). The calibration curve at these wavelengths was established as a function of La(III), Sm(III), Eu(III) and Gd(III) ions concentration with validity range from 5 to 50 mg L⁻¹. All experiments were performed in triplicates, and the reproducibility varied within ±1.5%.

The amount of equilibrium uptake of lanthanide ions is calculated by using the equation.

$$q_e = \frac{(C_0 - C_e)V}{m} \quad (1)$$

where q_e is the metal ion up taken by adsorbent mg g⁻¹, C_0 is the initial La(III), Sm(III), Eu(III) and Gd(III) ions concentration, C_e is these metal ions concentration (mg L⁻¹) after the adsorption process, m is the mass of adsorbent taken (g), V is the volume of metal ion solution taken (L). The percentage removal of these metal ions is defined as the ratio of the difference in metal ion concentration before and after adsorption ($C_0 - C_e$) to the initial concentration of the metal ion of the aqueous solution of the dye (C_0) and was calculated by using the equation.

$$\%R = \frac{(C_0 - C_e)}{C_0} \times 100 \quad (2)$$

The effect of adsorbent dose, pH, temperature and equilibrium isotherm and kinetic studies used for this study are given in the previous publication [27].

2.5. Determination of adsorption kinetics and isotherms and their statistical evaluation

Three adsorption isotherm models Langmuir [29], Freundlich [30] and D-R [31] were conducted in solution at a pH 5.0 with the initial metal ion concentration varied from 5–50 mg L⁻¹. Adsorption isotherms were obtained by plotting q_e vs. C_e . The Langmuir Eqs. (3) and (4), Freundlich Eq. (5) and D-R Eq. (6) equations were used to fit the adsorption isotherms of DE and DE-HDTMA for La(III), Sm(III), Eu(III) and Gd(III) ions.

$$q_e = \frac{q_{\max} K_L C_e}{1 + K_L C_e} \quad (3)$$

$$q_e = K_f C_e^{1/n} \quad (4)$$

$$q_e = q_{\max} \exp\left(-K_{DR} \left[RT \ln\left(1 + \frac{1}{C_e}\right)\right]^2\right) = q_{\max} \exp(-K_{DR} \varepsilon^2) \quad (5)$$

where q_e is the amount of metal ions taken up by the DE and DE-HDTMA (mg g⁻¹), q_{\max} is the monolayer capacity of adsorbent (mg g⁻¹), K_L is the Langmuir binding constant (L mg⁻¹), K_f is the Freundlich constant [mg g⁻¹(L mg⁻¹)^{1/n}] denoting adsorption capacity, n is the empirical constant, indicating of adsorption intensity, ε is the Polanyi potential which is equal to $RT \ln(1 + 1/C_e)$, K_{DR} is the constant related to the adsorption energy (mol²/kJ²), R and T is gas constant (8.314 J mol⁻¹ K⁻¹) and temperature (K), respectively, E_{DR} (kJ mol⁻¹) is the mean free energy of adsorption per molecule of adsorbate when it was transferred to the surface of solid from infinity in the solution, which provides information about the chemical or physical adsorption and can be determined according to the following equation:

$$E_{DR} = (2K_{DR})^{-1/2} \quad (6)$$

In the present work, the Lagergren pseudo-first-order [32] and pseudo-second-order kinetic models (9) [33] were used to fit the adsorption kinetic data obtained from metal

ions adsorption. In the adsorption kinetic experiments, the pH of the initial solution was fixed at a pH 5.0 for metal ions and the initial concentration of metal ion was 30 mg L⁻¹. Samples were collected at different time intervals. The kinetic curve was obtained by a plot of q_t vs. adsorption time.

$$q_t = q_e (1 - e^{-k_1 t}) \quad (7)$$

$$q_t = \frac{k_2 q_e^2 t}{1 + k_2 q_e t} \quad (8)$$

where q_e and q_t (mg g⁻¹) are the amount of metal ions adsorbed at equilibrium and at any time, respectively, k_1 is the pseudo-first-order rate constant (min⁻¹) and k_2 is the equilibrium rate constant of pseudo-second-order adsorption (g mg⁻¹ min⁻¹).

The fitness of the equilibrium and kinetic data were done using nonlinear methods, which were evaluated using the simplex method using the fitting facilities of the MicroCal Origin 2015 software. The suitability of the equilibrium and kinetic models were evaluated using a linear determination coefficient (R^2), chi-squared (χ^2) values and the error function ($F_{\text{error}\%}$). Error function of residues measures the differences between the theoretical and experimental amounts of metal ions adsorbed. Eqs. (10)–(12) are the mathematical expressions for respective R^2 , χ^2 and $F_{\text{error}\%}$, respectively [34].

$$R^2 = 1 - \frac{\sum (q_{e,\text{exp}} - q_{e,\text{cal}})^2}{\sum (q_{e,\text{exp}} - q_{e,\text{mean}})^2} = \frac{\sum (q_{e,\text{cal}} - q_{e,\text{mean}})^2}{\sum (q_{e,\text{cal}} - q_{e,\text{mean}})^2 + \sum (q_{e,\text{cal}} - q_{e,\text{exp}})^2} \quad (9)$$

$$\chi^2 = \sum \frac{(q_{e,\text{exp}} - q_{e,\text{cal}})^2}{q_{e,\text{cal}}} \quad (10)$$

$$F_{\text{error}\%} = 100 \times \sqrt{\frac{\sum \left[\frac{q_{e,\text{exp}} - q_{e,\text{cal}}}{q_{e,\text{exp}}} \right]^2}{N - P}} \quad (11)$$

In the above equations, $q_{e,\text{exp}}$ (mg g⁻¹) is the amount of metal ion uptake at equilibrium obtained from Eq. (1), $q_{e,\text{cal}}$ (mg g⁻¹) is the amount of metal ion uptake achieved from the models, and $q_{e,\text{mean}}$ (mg g⁻¹) is the mean of the $q_{e,\text{exp}}$ values, N is the number of experimental data points and P stands for number of parameters in the model.

3. Results and discussion

3.1. Characterization of adsorbents

The DE and DE-HDTMA samples were characterized using XRD, XRF, FTIR, SEM and energy-dispersive X-ray spectroscopy (EDS). The calculated CEC for DE was found to be 78.75 meq/100 g. The specific surface area value was found to be 42.2 m² g⁻¹ for DE and 23.0 m² g⁻¹ for DE-HDTMA. The BET surface area, the total pore volume, and the pore

diameter of DE and DE-HDTMA were found to be 9.95 m² g⁻¹, 0.47 m² g⁻¹, 0.045 cm³ g⁻¹, 0.006 cm³ g⁻¹, and 3.66 nm, 2.22 nm, respectively.

3.1.1. XRD analysis

The XRD patterns of DE and DE-HDTMA are presented in Fig. 1. These patterns look identical. However, after the addition of an organic HDTMABr modifier, the extra peaks at 2θ 18.20°, 21.45°, 22.00°, and 29.5° appeared, and the peaks at 2θ (17.8°), and (30.98°) disappeared. This is strong evidence of the modification which is carried out on the surface of DE. It could be explained that during the ion exchange mechanism, an amount of HBr was produced and then reacted with Na, Ca, Fe, and Mg ions forming minority phases and leached out from the DE and confirmed by XRF [25].

3.1.2. XRF analysis

The chemical composition of the DE and DE-HDTMA as determined by XRF technique (wt.%) is as follows, DE: SiO₂, 61.69; Al₂O₃, 20.74; Fe₂O₃, 8.32; K₂O, 4.01; MgO, 2.06; TiO₂, 1.13; Na₂O, 1.10; MgO, 2.06; Cl, 0.40; CaO, 0.21; P₂O₅, 0.15; SO₃, 0.11; BaO, 0.04; MnO, 0.02; NiO, 0.01. DE-HDTMA: SiO₂, 60.26; Al₂O₃, 23.22; Fe₂O₃, 8.65; K₂O, 3.89; MgO, 2.04; TiO₂, 1.18; Na₂O, 0.21; MgO, 2.06; Cl, 0.06; CaO, 0.15; P₂O₅, 0.16; SO₃, 0.08; BaO, 0.05; MnO, 0.03; NiO, 0.01. It seems from the chemical composition that the predominant exchangeable cation was sodium. According to XRF analysis, DE and DE-HDTMA are clay species which mainly consists of silicate, alumina and appreciable quantities of iron.

3.1.3. FTIR spectra

FTIR technique could be used to identify the major functional groups present in these two adsorbents. Fig. 2 shows the FTIR spectrum of DE, DE-HDTMA and HDTMABr. Both DE and DE-HDTMA show characteristic bands of DE. The absorption band at 3,623 cm⁻¹ is due to stretching vibrations of structural OH groups of diatomaceous earth. Large broadband at 1,086 cm⁻¹ is related to stretching vibrations of Si–O groups. The H₂O-stretching vibration was observed as broadband at 3,431 cm⁻¹. For DE-HDTMA, there appeared two new absorption bands at 2,920 and 2,851 cm⁻¹,

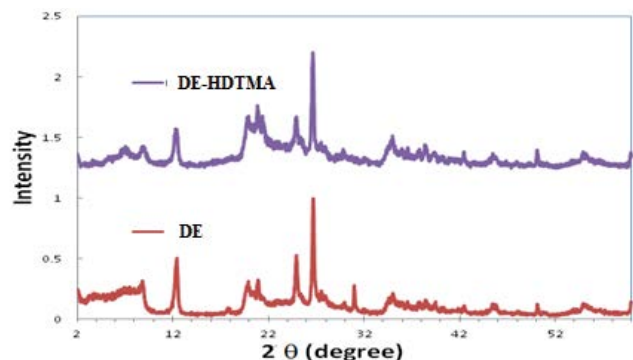


Fig. 1. X-ray diffraction patterns for DE and DE-HDTMA.

which represented the stretching vibrations of polymethylene groups (CH_2). These two characteristic bands are present in the FTIR spectrum of HDTMABr confirming the cationic exchange reaction between organic cation of the quaternary ammonium salt of surfactant and cations of DE.

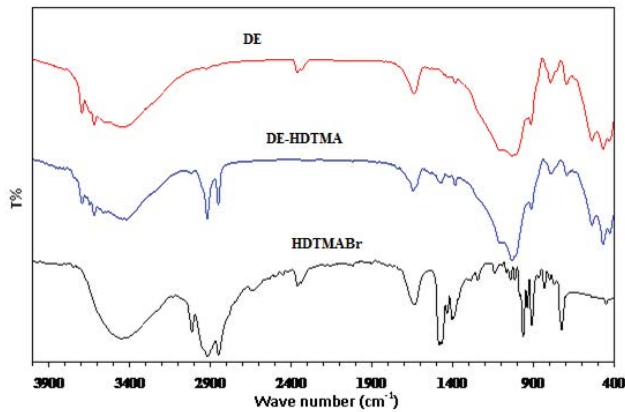


Fig. 2. Fourier-transform infrared spectra for DE, DE-HDTMA, and HDTMABr.

3.1.4. SEM observations

SEM micrographs for DE and DE-HDTMA are presented in Fig. 3. For DE it can be seen the presence of a hole in the surface as a form of a sieve. The porosity size as shown in Fig. 3c was reached on average 644 nm. The porosity of DE-HDTMA (Fig. 3b) became less due to the occurrence of the full interaction between DE and organic surfactant HDTMABr which covered the holes and pores.

3.1.5. Energy-dispersive X-ray spectroscopy

EDS chart gives a descriptive view of some chemical elements present in the DE before and after organic modification. The EDS for the DE and DE-HDTMA are shown in Fig. 4. The EDS gives the type and weight percent of each element present in the selected point of the sample at SEM micrographs. The percentage of each element after normalization is as follows, element, (%mass) DE: O, 69.25; Na, 1.73; Mg, 1.62; Al, 8.67; Si, 14.16; K, 1.37; Fe, 3.19. DE-HDTMA: C, 5.16; N, 9.54; O, 68.61; Na, 98; Mg, 1.05; Si, 11.60; K, 0.35; Fe, 1.24; Br, 1.49. It was noticed the differences between EDS analysis of DE and DE-HDTMA which are the appearance of new elements such as C and

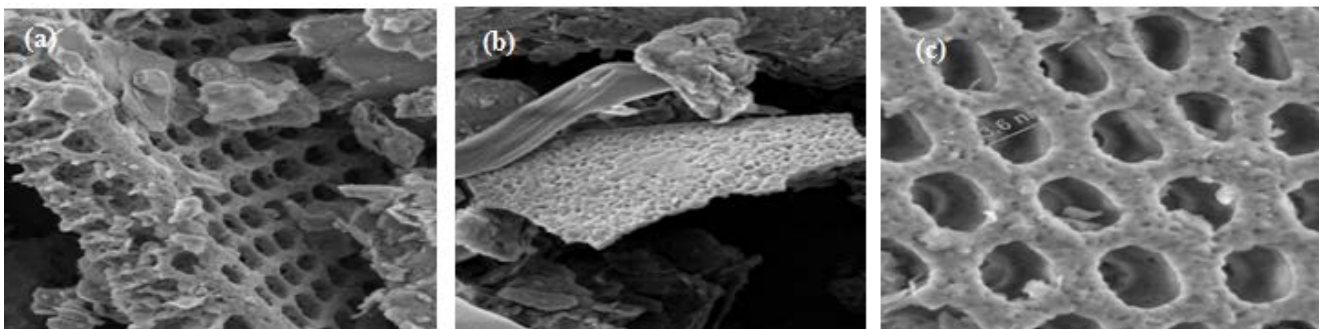


Fig. 3. Scanning electron micrographs for (a) DE, (b) DE-HDTMA, and (c) porosity dimension in DE.

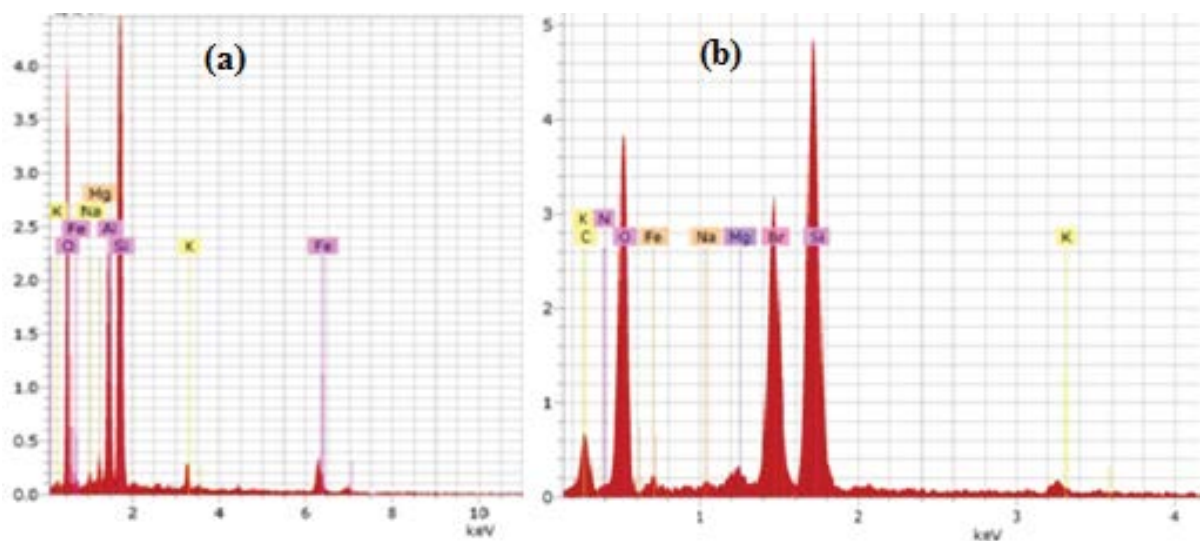


Fig. 4. Energy-dispersive X-ray spectroscopy for (a) DE and (b) DE-HDTMA.

N due to HDTMA, which resulted in the decrease in the percentage of Mg, Al and Si. This gives an indication of the presence of HDTMA on the surface of DE.

3.2. Effect of adsorbent dosage

The effect of DE and DE-HDTMA dosage (0.02–0.35 g) on metal ions adsorption was studied at pH 5.0 and 25°C and presented in Fig. 5. The removal percentage of metal ions extracted from the solution clearly increases with DE and DE-HDTMA content increasing at 0.2 g/50 mL, and only very slightly increases with solid content after that amount. Hence, the optimal dose is 0.2 g/50 mL for the four metal ions. The increase of metal ions adsorption is easily explained by an increase in the surface area and thus the metal-binding sites of DE and DE-HDTMA samples. This availability enhances the adsorption of metal ions from solution to solid keeping the initial concentration of metal ions constant with the increasing of DE and DE-HDTMA dose. The decrease in q_e for metal ions by DE and DE-HDTMA can be attributed to the fact that some of the adsorption sites remain unsaturated during the

adsorption process; whereas the number of available adsorption sites increases by an increase in adsorbent and this leads to an increase in removal efficiency. A similar trend was earlier reported in the literature for the removal of U(VI), Th(IV), Sm(III) and Nd(III) ions by diatomaceous earth and its organomodified form from aqueous solutions [27,28].

3.3. Effect of ionic strength

The effect of ionic strength on adsorption uptake of metal ions on the DE and DE-HDTMA surfaces was studied at a variable concentration of sodium chloride (0.01, 0.05, 0.10, 0.15 and 0.20 M). (Ionic strength (I) = 0.01, 0.05, 0.10, 0.15 and 0.20, respectively). The influence of ionic strength on the amount of metal ions adsorbed by DE and DE-HDTMA at pH 5.0 and 25°C was illustrated in Fig. S1. The results showed a decrease in the uptake amount of metal ions with the increase of electrolyte concentration (and hence the ionic strength). These results can be attributed to first, increasing Na^+ concentration and therefore increasing competition for the adsorption sites on the DE and DE-HDTMA, and second, decreasing activity

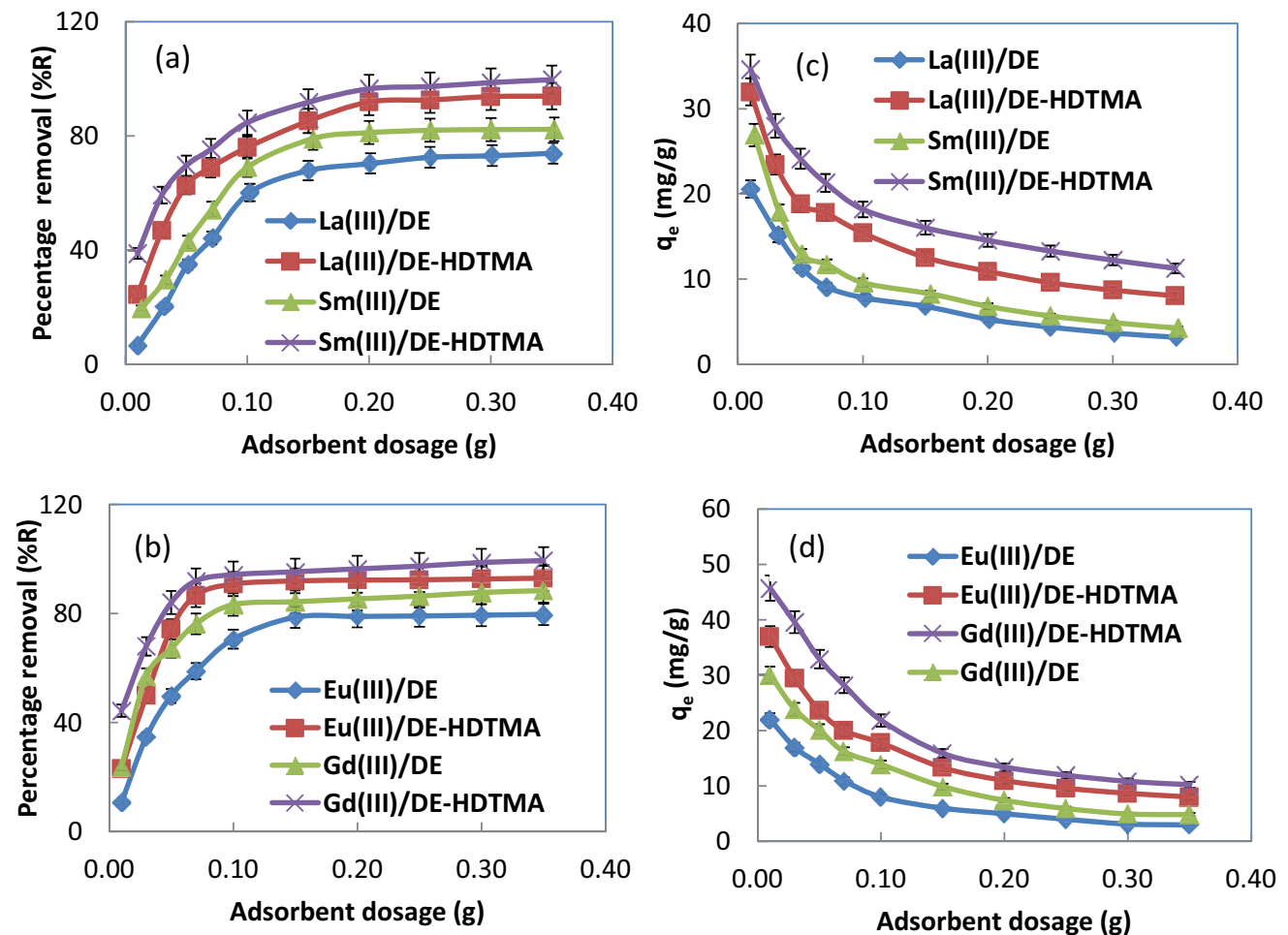


Fig. 5. Effect of adsorbent dosage on the DE and DE-HDTMA percentage removal for (a) La(III) and Sm(III) and (b) Eu(III) and Gd(III). Effect of adsorbent dosage on the DE and DE-HDTMA adsorption efficiency for (c) La(III) and Sm(III) and (d) Eu(III) and Gd(III). Initial metal ions concentration 30 mg L⁻¹; pH = 5.0; time of contact 24 h; temperature 25°C.

of metal ions in solution due to increasing non-ideality of solution. This non-ideality is due to increasing electrostatic interaction between Cl^- and La(III), Sm(III), Eu(III) and Gd(III) ions [28].

3.4. Effect of pH

The adsorption efficiency of adsorbents can be affected by a variety of parameters: The pH of metal ion solution plays an important role during the adsorption process and particularly affects the adsorption capacity. Fig. 6 shows the influence of pH on the adsorption of La(III), Sm(III), Eu(III) and Gd(III) ions on DE and DE-HDTMA. The study was carried out in the pH range of 2.0–7.0 keeping all other parameters constant. Alkaline conditions did not be studied to avoid complications from precipitation. Based on Fig. 5, it can be found that the adsorption of DE and DE-HDTMA for the metal ions had a similar change trend within the pH range studied. At low pH values, the hydrogen ion concentration is high; therefore, protons can compete with the lanthanide cations for surface sites. In addition, increasing the pH value would result in lower columbic repulsion of the adsorbed metal ions [35,36]. It is well known that the hydrolysis of trivalent lanthanides begins at low pH values and various species can be formed, such as $\text{Ln}(\text{OH})^{2+}$, $\text{Ln}(\text{OH})^+$, $\text{Ln}(\text{OH})_3$ and Ln^{3+} [37]. These hydrolyzed species, more hydrophobic than trivalent lanthanide cations, can be dehydrated and stick to the adsorbent surface [38]. This explains the slow increase in adsorption efficiency values in the 2–5 pH range, which is responsible for the formation of different surface complexes of trivalent lanthanide cations with silanol: $\text{Si}-\text{OH}$ and aluminol: $\text{Al}-\text{OH}$ groups exist in DE and DE-HDTMA surfaces. After pH 5, the hydrolysis precipitation most probably would start due to the formation of various hydrocomplexes in an aqueous solution leading to lower adsorption efficiency of these ions. Therefore, for further experiments, the pH was set to five to avoid any misinterpretation of the adsorption performance.

3.5. Effect of contact time and initial metal concentration

The equilibrium time has a crucial impact in the adsorption process, Fig. 7 shows plots of the adsorption uptake for La(III), Sm(III), Eu(III) and Gd(III) ions as a function of contact time (5–210 min) at a constant initial concentration of 30 mg L^{-1} . From the results, it is observed that with the increase in contact time up to 60 min, the removal efficiency for DE and DE-HDTMA was sharply increased and equilibrium was reached after 180 min. The quick adsorption rate of the four lanthanide ions on DE and DE-HDTMA was due to the higher surface area and easy accessibility of a large number of active sites [28].

The adsorption of metal ions onto DE and DE-HDTMA from an aqueous solution of different concentrations 10, 30 and 50 mg L^{-1} is presented in Fig. 8. The uptake increases with increasing metal ions concentration of the aqueous solutions. The adsorption capacity was increased with concentration increased from 10 to 30 to 50 mg L^{-1} from 70.912 to 119.934 to $163.934 \text{ mg L}^{-1}$ for La/DE, from 113.636 to 156.250 to $208.333 \text{ mg L}^{-1}$ for La/DE-HDTMA, from 78.125 to 185.185 to $303.030 \text{ mg L}^{-1}$ for Sm/DE, from

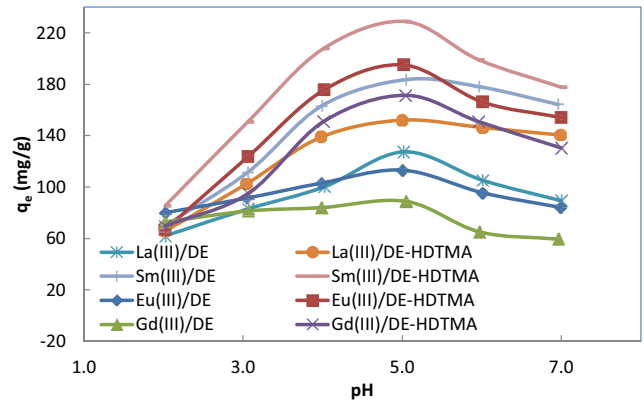


Fig. 6. Effect of pH on the DE and DE-HDTMA adsorption efficiency for La(III), Sm(III), Eu(III) and Gd(III). Initial metal ions concentration 30 mg L^{-1} ; adsorbent dosage $0.20 \text{ g}/50 \text{ mL}$; time of contact 24 h; temperature 25°C .

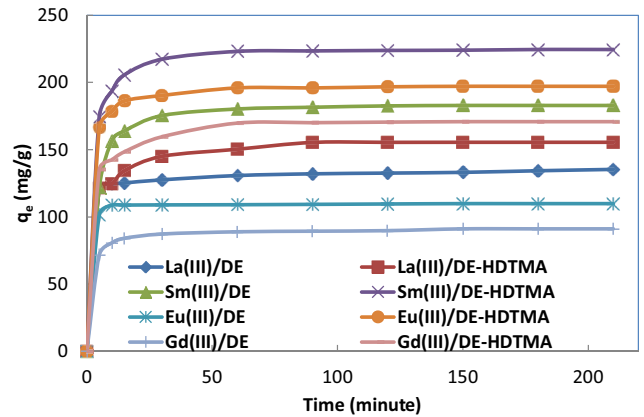


Fig. 7. Effect of contact time on the DE and DE-HDTMA adsorption efficiency for La(III), Sm(III), Eu(III) and Gd(III) ions. Initial metal ions concentration 30 mg L^{-1} ; pH = 5.0; adsorbent dosage $0.20 \text{ g}/50 \text{ mL}$; temperature 25°C .

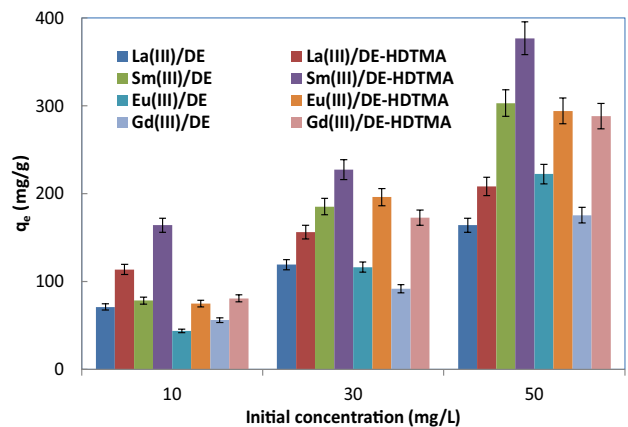


Fig. 8. Effect of initial metal concentration on the DE and DE-HDTMA adsorption efficiency for La(III), Sm(III), Eu(III) and Gd(III) ions. Initial metal ions concentration 30 mg L^{-1} ; pH = 5.0; adsorbent dosage $0.20 \text{ g}/50 \text{ mL}$; temperature 25°C .

163.934 to 227.272 to 373.852 mg L⁻¹ for Sm/DE-HDTMA, from 43.668 to 116.279 to 222.222 mg L⁻¹ for Eu/DE, from 74.672 to 196.078 to 294.118 mg L⁻¹ for Eu/DE-HDTMA, from 55.921 to 91.743 to 175.439 for Gd/DE and from 80.645 to 172.414 to 286.343 mg L⁻¹ for Gd/DE-HDTMA, respectively. These findings show that energetically more favorable sites are involved in increasing concentrations of the metal ions. Thus, high concentrations of these ions in feed mean faster adsorption and greater system efficiency [27]. It can be seen in Fig. 7 that DE and DE-HDTMA had the highest removal of these four metal ions at high concentrations of 50 mg L⁻¹. This can be adduced to the fact that the concentration gradient of metal ions is directly proportional to the initial concentration and the increase in the transfer of metal ions from the solution to the adsorbent material was due to the increase in driving force [39].

3.6. Adsorption isotherms

The adsorption isotherms, Langmuir Eqs. (3) and (4), Freundlich Eq. (5) and D-R Eqs. (6) and (7), were studied in order to understand the type of interaction between adsorbent and adsorbate for adsorption process and to determine the adsorption efficiency and the nature of metal ions adsorption. The adsorption isotherm parameters together with R^2 , χ^2 , and $F_{\text{error}\%}$ fitted by the Langmuir, Freundlich and D-R models were summarized in Table 1 and presented in Figs. S2 and S3. These figures showed that with the increase of equilibrium concentration in the system, the equilibrium adsorption efficiency of DE and DE-HDTMA for these four metal ions increased gradually, and it stabilized when the equilibrium mass concentration

was ≈ 45 mg L⁻¹. The high regression coefficient R^2 values (0.9907–0.9975), (0.9725–0.9959) and (0.9919–0.9999), low χ (0.028–0.918), (0.175–1.465) and (0.008–0.527) and low $F_{\text{error}\%}$ (1.495–5.586) for Langmuir, Freundlich and D-R isotherm models, respectively show good fitting of the data obtained, which follows that La(III), Sm(III), Eu(III) and Gd(III) ions adsorption fits the three isotherm models. The applicability of the three isotherm models to the all investigated systems implies that both monolayer adsorption and heterogeneous surface conditions exist under the experimental conditions studied. The adsorption of these four metal ions on the DE and DE-HDTMA surfaces is thus complex, involving more than one mechanism. The Freundlich isotherm model data gave n values greater than 1, which revealed that there was favorable adsorption. Maximum adsorption capacities (q_{max}) for La(III), Sm(III), Eu(III) and Gd(III) ions by DE and DE-HDTMA at 25°C were obtained to be 185.185, 232.558; 117.647, 199.601; 111.048, 172.414 and 92.593 and 156.250 mg L⁻¹, respectively.

Adsorption capacities q_{max} and the mean free energies of adsorption E_{DR} (kJ mol⁻¹) are calculated from D-R isotherm for the four metal cations, Table 1. The adsorption is driven by physical forces if the value of E_{DR} is less than 8 (kJ mol⁻¹), is driven by chemical ion-exchange if E_{DR} is between 8–16 (kJ mol⁻¹) and is driven by particle diffusion if the value of E_{DR} is greater than 16 (kJ mol⁻¹) [40]. It was seen that all the experimental E_{DR} value ranged between 0.858–2.887 kJ mol⁻¹, which clearly demonstrates the physical adsorption of La(III), Sm(III), Eu(III) and Gd(III) ions adsorbed onto DE and DE-HDTMA surfaces. The difference in q_{max} derived from the Langmuir and D-R models may be attributed to the different definitions of q_{max} in the two

Table 1

Langmuir, Freundlich and D-R isotherm constants for the adsorption of La(III), Sm(III), Eu(III) and Gd(III) ions on DE and DE-HDTMA. Initial metal ions concentration 10–50 mg L⁻¹; pH = 5.0; adsorbent dosage 0.20 g/50 mL; temperature 25°C

Adsorbent	La/DE	La/DE-HDTMA	Sm/DE	Sm/DE-HDTMA	Eu/DE	Eu/DE-HDTMA	Gd/DE	Gd/DE-HDTMA
Langmuir isotherm								
q_{max} (mg g ⁻¹)	185.185	232.558	117.647	199.601	111.048	172.414	92.593	156.250
K_L (L mg ⁻¹)	0.017	0.077	0.029	0.012	0.025	0.017	0.032	0.014
R^2	0.9969	0.9975	0.9907	0.9980	0.9978	0.9976	0.9966	0.9993
χ^2	0.141	0.121	0.096	0.061	0.918	0.824	0.226	0.11
$F_{\text{error}\%}$	2.23	1.56	1.76	1.49	5.59	3.26	2.51	1.49
Freundlich isotherm								
K_f (L g ⁻¹)	5.234	3.066	5.787	4.572	4.528	5.068	5.335	3.085
n	1.400	2.066	1.562	1.419	1.416	1.422	1.617	1.283
R^2	0.9873	0.9959	0.9725	0.9910	0.9797	0.9824	0.9808	0.9919
χ^2	1.079	0.981	1.121	0.629	1.465	0.175	0.995	0.6883
$F_{\text{error}\%}$	7.013	4.39	6.45	5.09	8.03	1.31	5.42	4.49
D-R isotherm								
q_{max} (mg g ⁻¹)	87.575	182.911	89.756	91.836	53.016	113.228	55.556	72.799
E (kJ mol ⁻¹)	1.244	2.283	2.887	2.858	2.643	0.621	0.816	2.071
R^2	0.9998	0.9919	0.9963	0.9999	0.9993	0.9919	0.9991	0.9997
χ^2	0.062	0.418	0.085	0.061	0.527	0.441	0.008	0.028
$F_{\text{error}\%}$	2.127	2.81	2.94	2.59	4.62	2.25	0.65	0.91

models. In Langmuir, q_{\max} represents maximum adsorption of metal ions at monolayer coverage, whereas the D-R represents the maximum adsorption of metal ions at the total specific micropores volume of the adsorbent. Thereby, the value of q_{\max} derived from the Langmuir model is larger than that derived from the D-R model [41].

It is clear from the values of q_{\max} (Table 1) that the organically modified clay (DE-HDTMA) is much more efficient adsorbents of metal ions than the unmodified clay (DE). Clays that are organically modified with long-chain organic cations such as hexadecyltrimethylammonium surfactant used in this work are often referred to as “partitioning complexes”. The mechanism in DE and in their adsorbent complexes is considered to be of the surface adsorption type; hence has a limited capacity due to the finite surface area available. On the other hand the mechanism for “partitioning complexes” is considered to be organic partitioning; hence has no such limitation. This explains the higher values of q_{\max} of the surfactant-modified clay in comparison to the unmodified clay [42]. Also from the values of the q_{\max} it can be concluded that the capacity of adsorption of DE and DE-HDTMA surfaces

for these metal cations follows the sequence, La(III) > Sm(III) > Eu(III) > Gd(III). An adsorbent’s affinity to a particular ion can correlate with its atomic mass, electronegativity, and ionic radii [43]. This pattern is observed by the adsorption capacity sequences for those four metal ions. Similar observations have been reported by many researchers [17,44–47] for the adsorption of La(III), Sm(III), Eu(III) and Gd(III) ions by different adsorbents.

Adsorption of REEs on an adsorbent is a complex process where multiple mechanisms, such as ion-exchange, surface complexation, and electrostatic interactions take place simultaneously. The description of the adsorption mechanism for REEs onto DE and DE-HDTMA could occur via surface complexation between REEs and deprotonated carboxylic and silica groups and active sites on DE via ion exchange or chelation. The mechanism for “partitioning complexes” in case of DE-HDTMA is considered to be organic partitioning; due to molecular electrostatic interactions.

The comparisons of DE and DE-HDTMA adsorbents with other materials reported in the literature [18,12,40,48–59], (Table 2) show that those two adsorbents are

Table 2

Comparison between the maximum monolayer adsorption capacity (q_{\max} , mg g⁻¹) of La(III), Sm(III), Eu(III) and Gd(III) ions on various adsorbents

Adsorbent	Adsorbate	Conditions		q_{\max} (mg g ⁻¹)	Reference
		pH	T (°C)		
Banana peels biochar	La(III)	5.2	25	47.8	[18]
	Gd(III)			52.6	
Magnetic nano-hydroxyapatite	Sm(III)	5.5	25	370	[48]
Dimethacrylate–methacrylic acid copolymers	Gd(III)	6.0	20	19.4	[49]
Organomodified bentonite	Sm(III)	4.0	25	17.7	[50]
Fe-modified biochar	Eu(III)	6.0	22	9.8	[40]
Granular hybrid hydrogel	La(III)	6.0	25	269.37	[51]
	La(III)			19.46	
Organomodified red clay	Eu(III)	6.0	25	41.21	[52]
	La(III)			47.67	
Ethylenediaminetetraacetic acid (EDTA)- β-cyclodextrin	Eu(III)	4.0	25	55.48	[53]
	Eu(III)			125.63	
Lewis base ligand	Sm(III)	4.0	25	124.38	[12]
	Eu(III)			34.96	
Marine sediments	Eu(III)	8.0	25	34.96	[54]
Silica-urea–formaldehyde composite	Eu(III)	5.0	25	52.33	[55]
Cysteine – chitosan magnetic nanoparticle	La(III)	5.0	27	16.0	[56]
Chitosan/carbon composite	Gd(III)	7.0	20	79.84	[57]
Animal–plant biosorbent	La(III)	6.0	50	200	[58]
No-silica monolith hybrid adsorbent	Eu(III)	4.0	25	163.13	[59]
	La(III)			185.185	
	Sm(III)			117.647	
	Eu(III)			111.048	
	Gd(III)			92.593	
DE	La(III)	5.0	25	232.558	This work
	Sm(III)			199.601	
	Eu(III)			172.414	
	Gd(III)			156.250	
DE-HDTMA	Sm(III)	5.0	25	199.601	This work
	Eu(III)			172.414	
	Gd(III)			156.250	

potential effective for the removal of La(III), Sm(III), Eu(III) and Gd(III) ions from aqueous solution.

3.7. Adsorption kinetics

Pseudo-first-order kinetic and pseudo-second-order kinetic models were used to fit the adsorption kinetics of the process and the results were shown in Figs. S4 and S5. The fitting parameters were given in Table 3, R^2 (>0.9999), χ^2 (<0.834) and $F_{\text{error}\%}$ (<1.99) values were found to be best fitted for pseudo-second-order kinetic model compared to pseudo-first-order kinetic model R^2 (>0.7382), χ^2 (<29.716) and $F_{\text{error}\%}$ (<14.03). In addition, the equilibrium adsorption capacity obtained by fitting the pseudo-second-order kinetic equation was closer to the equilibrium adsorption capacity obtained in the experiment. Therefore, the pseudo-second-order kinetic model can better reflect the adsorption process of DE and DE-HDTMA for La(III), Sm(III), Eu(III) and Gd(III) ions. According to the mechanism developed by the pseudo-second-order kinetic model, the process of adsorption could be carried on because of the availability of the adsorption sites rather than the concentration of metal ions [60].

3.8. Adsorption thermodynamics

The activation energy (E_a in kJ mol^{-1}) may be defined as the minimum amount of energy required to adsorption process proceeds, and it was calculated from the Arrhenius equation:

$$\ln k_2 = \ln A - \frac{E_a}{RT} \quad (12)$$

where k_2 ($\text{g mg}^{-1} \text{min}^{-1}$): the rate constant of the pseudo-second-order kinetic model in an adsorption system of the

four metal ions for DE and DE-HDTMA, T (K): temperature and R : gas constant ($8.314 \text{ kJ mol}^{-1}$), A plot of $\ln k_2$ vs. $1/T$ yields a straight line (Fig. S6) with slope $-E_a/R$ is obtained.

The thermodynamic parameters are one of the indispensable instruments in the prediction of the adsorption system, whether it is a physisorption or chemisorption method. The thermodynamic parameters could be calculated from the following laws of thermodynamics:

$$\Delta G^\circ = -RT \ln K_d \quad (13)$$

where K_d for the adsorption reaction can be defined [61]:

$$K_d = \frac{q_e}{C_e} \quad (14)$$

Values of K_d are obtained by plotting $\ln q_e/C_e$ vs. q_e and extrapolating q_e to zero.

$$\Delta G^\circ = \Delta H^\circ - T \Delta S^\circ \quad (15)$$

$$\ln K_d = -\frac{\Delta H^\circ}{RT} + \frac{\Delta S^\circ}{R} \quad (16)$$

where ΔG° (kJ mol^{-1}): standard Gibbs free energy change, K_d : equilibrium constant, ΔH° (kJ mol^{-1}): enthalpy change, ΔS° (kJ mol^{-1}): entropy change. Predictions of the intercept and slope of the linear plot of $\ln K_d$ vs. $1/T$ (Fig. S7) give, respectively, ΔS° and ΔH° values.

The values of ΔG° , ΔH° , ΔS° and E_a for the adsorption of La(III), Sm(III), Eu(III) and Gd(III) ions onto DE and DE-HDTMA are given in Table 4. The negative values of ΔG° suggest that the adsorption of metal ions occurred favorably and spontaneously with low requirements for adsorption energy. The negative values of ΔH° for DE and

Table 3

Pseudo-first-order and pseudo-second-order adsorption rate constants and calculated $q_{e,\text{cal}}$ and experimental $q_{e,\text{exp}}$ values for the adsorption of La(III), Sm(III), Eu(III) and Gd(III) ions onto DE and DE-HDTMA. Initial metal ions concentration $10\text{--}50 \text{ mg L}^{-1}$; pH = 5.0; adsorbent dosage $0.20 \text{ g}/50 \text{ mL}$; temperature 25°C

System	La/DE	La/DE-HDTMA	Sm/DE	Sm/DE-HDTMA	Eu/DE	Eu/DE-HDTMA	Gd/DE	Gd/DE-HDTMA
$q_{e,\text{exp}}$ (mg g^{-1})	185.185	232.558	117.647	199.601	111.048	172.414	92.593	156.250
Pseudo-first-order								
$q_{e,\text{cal}}$ (mg g^{-1})	81.101	130.632	95.231	153.879	88.637	137.759	63.236	113.511
k_1 (min^{-1})	0.041	0.031	0.010	0.031	0.017	0.036	0.021	0.017
R^2	0.8802	0.8554	0.7817	0.7382	0.7718	0.7789	0.7990	0.7661
χ^2	35.853	36.559	35.978	47.145	55.237	61.918	29.716	57.245
$F_{\text{error}\%}$	19.49	14.789	20.764	23.33	41.17	33.25	14.03	23.33
Pseudo-second-order								
$q_{e,\text{cal}}$ (mg g^{-1})	184.502	227.237	116.279	197.978	110.906	171.821	91.743	155.763
k_2 ($\text{g mg}^{-1} \text{min}^{-1}$)	0.002	0.004	0.035	0.007	0.024	0.011	0.008	0.069
R^2	0.9998	0.9993	0.9998	0.9994	0.9997	0.9996	0.9998	0.9996
χ^2	0.219	0.594	0.119	0.029	0.035	0.528	0.834	0.067
$F_{\text{error}\%}$	1.24	1.99	1.08	1.56	0.59	1.90	0.65	0.69

Table 4
Thermodynamic parameters for the adsorption of La(III), Sm(III), Eu(III) and Gd(III) ions onto DE and DE-HDTMA

T (K)	$-\Delta G$ (kJ mol ⁻¹)	$-\Delta H$ (kJ mol ⁻¹)	$-\Delta S$ (kJ mol ⁻¹)	E_a (kJ mol ⁻¹)
La(III)/DE				
298	6.368			
308	4.735	40.932	116.429	7.182
318	4.060			
La(III)/DE-HDTMA				
298	1.093			
308	0.933	6.109	17.459	27.302
318	0.756			
Sm(III)/DE				
298	4.464			
308	3.748	28.442	80.322	23.562
318	2.854			
Sm(III)/DE-HDTMA				
298	2.209			
308	1.750	14.293	40.586	26.177
318	1.399			
Eu(III)/DE				
298	4.427			
308	3.769	29.902	85.235	23.130
318	2.714			
Eu(III)/DE-HDTMA				
298	5.363			
308	4.655	26.991	72.515	10.437
318	3.912			
Gd(III)/DE				
298	7.498			
308	7.125	19.002	38.569	21.267
318	6.726			
Gd(III)/DE-HDTMA				
298	6.131			
308	5.337	22.831	56.261	18.386
318	5.015			

DE-HDTMA, indicating that the adsorption processes were exothermic. Moreover, the decrease of ΔG° values with increasing the temperature from 298 to 318 K asserted the exothermicity of the adsorption process, which was also confirmed by the negative value of ΔH° . In addition, the negative values of ΔS° reflect a decrease in the degree of freedom of metal ions on the solid-solution interface of the adsorbents. The magnitude of activation energy gives a type of adsorption, which is mainly physical or chemical. The range of 5–40 kJ mol⁻¹ of activation energy corresponds to a physisorption mechanism [62]. The activation energy values obtained by this study are calculated between 7.182 and 27.302 kJ mol⁻¹ (Table 4) indicating that

the adsorption has a low potential barrier and is assigned to physisorption. These results are in good agreement with that obtained above from the calculation of mean free energies of adsorption (E_{DR}) using D-R isotherm.

4. Conclusions

In this study, the adsorption properties of naturally available low-cost diatomaceous earth (DE) and its organo-modified form (DE-HDTMA) for La(III), Sm(III), Eu(III) and Gd(III) ions in solution were investigated. Based on R^2 , χ^2 , and $F_{\text{error}\%}$ values, the adsorption equilibrium data were best fitted by the Langmuir, Freundlich and D-R

isotherms. The maximum adsorption (q_{max}) capacities of DE and DE-HDTMA for metal ions were found to be 185.185, 232.558, 117.647, 199.60, 111.048, 172.414, 92.593 and 156.250 mg g⁻¹, respectively. The adsorption capacity was higher for DE-HDTMA (1.26–1.80 times) as compared with the raw DE. Moreover, the results of the D-R isotherm model suggest that the adsorption process was dominated by physisorption mechanisms. The kinetic experiments have shown that it is in best agreement with the model of pseudo-second-order, where the process was spontaneous and exothermic in nature. These results indicate that DE and DE-HDTMA might serve as an efficient, simple, and low-cost material for lanthanides metal ions removal from wastewaters.

References

- [1] H. Moriwaki, R. Koide, R. Yoshikawa, Y. Warabino, H. Yamamoto, Adsorption of rare earth ions onto the cell walls of wild-type and lipoteichoic acid-defective strains of *Bacillus subtilis*, *Appl. Microbiol. Biotechnol.*, 97 (2013) 3721–3728.
- [2] M.R. Awual, T. Yaita, S.A. El-Safty, H. Shiwaku, S. Suzuki, Y. Okamoto, Copper(II) ions capturing from water using ligand modified a new type mesoporous adsorbent, *Chem. Eng. J.*, 221 (2013) 322–330.
- [3] J. Roosen, K. Binnemans, Adsorption and chromatographic separation of rare earths with EDTA- and DTPA-functionalized chitosan biopolymers, *J. Mater. Chem. A*, 2 (2014) 1530–1540.
- [4] N. Freslon, G. Bayon, D. Birot, C. Bollinger, J.A. Barrat, Determination of rare earth elements and other trace elements (Y, Mn, Co, Cr) in seawater using Tm addition and Mg(OH)₂ co-precipitation, *Talanta*, 85 (2011) 582–587.
- [5] V. Hatje, K.W. Bruland, A.R. Flegal, Determination of rare earth elements after pre-concentration using NOBIAS-chelate PA-1 resin: method development and application in the San Francisco Bay plume, *Mar. Chem.*, 160 (2014) 34–41.
- [6] F. Xie, T.A. Zhang, D. Dreisinger, F. Doyle, A critical review on solvent extraction of rare earths from aqueous solutions, *Miner. Eng.*, 56 (2014) 10–28.
- [7] M.R. Awual, M.M. Hasan, Novel conjugate adsorbent for visual detection and removal of toxic lead(II) ions from water, *Microporous Mesoporous Mater.*, 196 (2014) 261–269.
- [8] M.R. Awual, G.E. Eldesoky, T. Yaita, Mu. Naushad, H. Shiwaku, Z.A. AlOthman, S. Suzuki, Schiff based ligand containing nano-composite adsorbent for optical copper(II) ions removal from aqueous solutions, *Chem. Eng. J.*, 279 (2015) 639–647.
- [9] A. Shahat, M.R. Awual, M.A. Khaleque, M.Z. Alam, Mu. Naushad, A.M.S. Chowdhury, Large-pore diameter nano-adsorbent and its application for rapid lead(II) detection and removal from aqueous media, *Chem. Eng. J.*, 273 (2015) 286–295.
- [10] I. Anastopoulos, A. Bhatnagar, E.C. Lima, I. Anastopoulos, A. Bhatnagar, E.C. Lima, Adsorption of rare earth metals: a review of recent literature, *J. Mol. Liq.*, 221 (2016) 954–962.
- [11] E.L. Afonso, L. Carvalho, S. Fateixa, C.O. Amorim, V.S. Amaral, C. Vale, E. Pereira, C.M. Silva, T. Trindade, C.B. Lopes, Can contaminated waters or wastewater be alternative sources for technology-critical elements? The case of removal and recovery of lanthanides, *J. Hazard. Mater.*, 380 (2019) 120845, <https://doi.org/10.1016/j.jhazmat.2019.120845>.
- [12] M.R. Awual, T. Kobayashi, Y. Miyazaki, R. Motokawa, H. Shiwaku, S. Suzuki, Y. Okamoto, T. Yaita, Selective lanthanide sorption and mechanism using novel hybrid Lewis base (*N*-methyl-*N*-phenyl-1,10-phenanthroline-2-carboxamide) ligand modified adsorbent, *J. Hazard. Mater.*, 252–253 (2013) 313–320.
- [13] M.R. Awual, N.H. Alharthi, Y. Okamoto, M.R. Karim, M.E. Halim, M.M. Hasan, M.M. Rahman, M.M. Islam, M.A. Khaleque, M.C. Sheikh, Ligand field effect for Dysprosium(III) and Lutetium(III) adsorption and EXAFS coordination with novel composite nanomaterials, *Chem. Eng. J.*, 320 (2017) 427–435.
- [14] A. Alshameri, H.P. He, C. Xin, J.X. Zhu, W. Xinghu, R.L. Zhu, H.L. Wang, Understanding the role of natural clay minerals as effective adsorbents and alternative source of rare earth elements: adsorption operative parameters, *Hydrometallurgy*, 185 (2019) 149–161.
- [15] F. Alakhras, Kinetic studies on the removal of some lanthanide ions from aqueous solutions using amidoxime-hydroxamic acid polymer, *J. Anal. Methods Chem.*, 2018 (2018) 1–7, <https://doi.org/10.1155/2018/4058503>.
- [16] M. Khalil, T.Y. Mohamed, A. El-Tantawy, Kinetic evaluations for the sorption process of lanthanide ions with poly-*o*-toluidine Zr(IV) tungstophosphate, *J. Inorg. Organomet. Polym. Mater.*, 27 (2017) 757–769.
- [17] E. Kusriani, D.D. Kinastiti, L.D. Wilson, A. Usman, A. Rahman, Adsorption of lanthanide ions from an aqueous solution in multicomponent systems using activated carbon from banana peels (*Musa Paradisiaca* L.), *Int. J. Technol.*, 9 (2018) 1132–1139.
- [18] O.A. Oyewo, M.S. Onyango, C. Wolkersdorfer, Lanthanides removal from mine water using banana peels nanosorbent, *Int. J. Environ. Sci. Technol.*, 15 (2018) 1265–1274.
- [19] A. Lozano, C. Ayora, A. Fernández-Martínez, Sorption of rare earth elements onto basaluminite: the role of sulfate and pH, *Geochim. Cosmochim. Acta*, 258 (2019) 50–62.
- [20] H.E. Rizk, M.F. Attallah, A.M.I. Ali, Investigations on sorption performance of some radionuclides, heavy metals and lanthanides using mesoporous adsorbent material, *J. Radioanal. Nucl. Chem.*, 314 (2017) 2475–2487.
- [21] W.R. Mohamed, S.S. Metwally, H.A. Ibrahim, E.A. El-Sherief, H.S. Mekhamer, I.M.I. Moustafa, E.M. Mabrouk, Impregnation of task-specific ionic liquid into a solid support for removal of neodymium and gadolinium ions from aqueous solution, *J. Mol. Liq.*, 236 (2017) 9–17.
- [22] S. Fields, Z. Korunic, A. McLaughlin, T. Stathers, Standardized Testing for Diatomaceous Earth, Proceedings of the 8th International Conference on Stored-Product Protection, CAB International, Wallingford, United Kingdom, 2003, pp. 779–784.
- [23] H.E.G.M. Mohamed Bakr, Diatomite: its characterization, modifications and applications, *Asian J. Mater. Sci.*, 2 (2010) 121–136.
- [24] U.F. Al-Karam, A.F. Danil deNamor, G.A.W. Derwish, A.H. Al-Dujaili, Removal of chromium, copper, cadmium and lead ions from aqueous solutions by diatomaceous earth, *Environ. Eng. Manage. J.*, 11 (2012) 811–819.
- [25] R.Z. Al Bakain, R.A. Abu-Zurayk, I. Hamadneh, F.I. Khalili, A.H. Al-Dujaili, A study on removal characteristics of *o*-, *m*-, and *p*-nitrophenol from aqueous solutions by organically modified diatomaceous earth, *Desal. Water Treat.*, 56 (2014) 826–838.
- [26] R.A. Abu-Zurayk, R.Z. Al Bakain, I. Hamadneh, A.H. Al-Dujaili, Adsorption of Pb(II), Cr(III) and Cr(VI) from aqueous solution by surfactant-modified diatomaceous earth: equilibrium, kinetic and thermodynamic modeling studies, *Int. J. Miner. Process.*, 140 (2015) 79–87.
- [27] S.I.Y. Salameh, F.I. Khalili, A.H. Al-Dujaili, Removal of U(VI) and Th(IV) from aqueous solutions by organically modified diatomaceous earth: evaluation of equilibrium, kinetic and thermodynamic data, *Int. J. Miner. Process.*, 168 (2017) 9–18.
- [28] I. Hamadneh, A. Alatawi, R. Zalloum, R. Albuqain, S. Alstori, F.I. Khalili, A.H. Al-Dujaili, Comparison of Jordanian and standard diatomaceous earth as an adsorbent for removal of Sm(III) and Nd(III) from aqueous solution, *Environ. Sci. Pollut. Res.*, 26 (2019) 20969–20980.
- [29] I. Langmuir, The adsorption of gases on plane surface of glass, mica and platinum, *J. Am. Chem. Soc.*, 40 (1918) 1361–1403.
- [30] H.M.F. Freundlich, About the adsorption, *Zeitschrift für Physikalische Chemie*, 57 (1906) 385–470.
- [31] M.M. Dubinin, E.D. Zaverina, L.V. Radushkevich, Sorption and structure of active carbon I. adsorption of organic vapors, *J. Phys. Chem. A*, 21 (1947) 1351–1362.
- [32] S. Lagergren, About the theory of so-called adsorption of soluble substances, *Kungliga Svenska Vetenskapsakademiens Handlingar*, 24 (1898) 1–39.

- [33] Y.-S. Ho, Review of second-order models for adsorption systems, *J. Hazard. Mater.*, 136 (2006) 681–689.
- [34] E.C. Lima, M.A. Adebayo, F.M. Machado, Chapter 3 – Kinetic and Equilibrium Models of Adsorption, C.P. Bergmann, F. Machado, Eds., *Carbon Nanomaterials as Adsorbents for Environmental and Biological Applications*, Springer, New York, 2015, pp. 33–69.
- [35] A.A.H. Faisal, M.D. Ahmed, Removal of copper ions from contaminated groundwater using waste foundry sand as permeable reactive barrier, *Int. J. Environ. Sci. Technol.*, 12 (2015) 2613–2622.
- [36] D.L. Ramasamy, V. Puhakka, B. Doshi, S. Iftakhar, M. Sillanpää, Fabrication of carbon nanotubes reinforced silica composites with improved rare earth elements adsorption performance, *Chem. Eng. J.*, 365 (2019) 291–304.
- [37] M.R. Awual, T. Yaita, H. Shiwaku, Design a novel optical adsorbent for simultaneous ultra-trace cerium(III) detection, sorption and recovery, *Chem. Eng. J.*, 228 (2013) 327–335.
- [38] T. Xiaoli, R. Xuemei, C. Changlun, W. Xiangke, Analytical approaches to the speciation of lanthanides at solid-water interfaces, *TrAC Trends Anal. Chem.*, 61 (2014) 107–132.
- [39] M.-W. Wan, C.-C. Wang, C.-M. Chen, The adsorption study of copper removal by chitosan-coated sludge derived from water treatment plant, *J. Environ. Manage.*, 4 (2013) 545–551.
- [40] V. Frišták, B. Micháleková-Richveisová, E. Víglašová, L. Ďuriška, M. Galamboš, E. Moreno-Jiménez, M. Pipiška, G. Soja, Sorption separation of Eu and As from single-component systems by Fe-modified biochar: kinetic and equilibrium study, *J. Iran Chem. Soc.*, 14 (2017) 521–530.
- [41] D. Xu, X.L. Tan, C.L. Chen, X.K. Wang, Adsorption of Pb(II) from aqueous solution to MX-80 bentonite: effect of pH, ionic strength, foreign ions and temperature, *Appl. Clay Sci.*, 41 (2008) 37–46.
- [42] Z. Rawajfih, N. Nsour, Characteristics of phenol and chlorinated phenols sorption onto surfactant-modified bentonite, *J. Colloid Interface Sci.*, 298 (2006) 39–49.
- [43] K. Vijayaraghavan, M. Sathishkumar, R. Balasubramanian, Interaction of rare earth elements with a brown marine alga in multi-component solutions, *Desalination*, 265 (2011) 54–59.
- [44] M.S. Hagag, A.M.A. Morsy, A.H. Ali, A.S. El-Shiekh, Adsorption of rare earth elements onto the Phosphogypsum a waste by-product, *Water Air Soil Pollut.*, 230 (2019) 308, <https://doi.org/10.1007/s11270-019-4362-z>.
- [45] F. Granados-Correa, J. Vilchis-Granados, M. Jiménez-Reyes, L.A. Quiroz-Granados, Adsorption behaviour of La(III) and Eu(III) ions from aqueous solutions by hydroxyapatite: kinetic, isotherm, and thermodynamic studies, *J. Chem.*, 2013 (2013) 1–9.
- [46] J.W. Tang, K.H. Johannesson, Adsorption of rare earth elements onto Carrizo sand: experimental investigations and modeling with surface complexation, *Geochim. Cosmochim. Acta*, 69 (2005) 5247–5261.
- [47] T. Prasada Rao, V.M. Biju, Trace determination of lanthanides in metallurgical, environmental, and geological samples, *Crit. Rev. Anal. Chem.*, 30 (2000) 179–220.
- [48] C. Gok, Neodymium and samarium recovery by magnetic nano-hydroxyapatite, *J. Radioanal. Nucl. Chem.*, 301 (2014) 641–651.
- [49] Z.Y. Bunina, K. Brylev, O. Yurchenko, Sorption materials based on ethylene glycol dimethacrylate and methacrylic acid copolymers for rare earth elements extraction from aqueous solutions, *Adsorpt. Sci. Technol.*, 35 (2017) 545–559.
- [50] D. Li, X.J. Chang, Z. Hu, Q.H. Wang, R.J. Li, X.L. Chai, Samarium(III) adsorption on bentonite modified with *N*-(2-hydroxyethyl) ethylenediamine, *Talanta*, 83 (2011) 1742–1747.
- [51] Y.F. Zhu, Y. Zheng, A.Q. Wang, A simple approach to fabricate granular adsorbent for adsorption of rare elements, *Int. J. Biol. Macromol.*, 72 (2015) 410–420.
- [52] A. Gladysz-Plaska, M. Majdan, E. Grabias, Adsorption of La, Eu and Lu on raw and modified red clay, *J. Radioanal. Nucl. Chem.*, 301 (2014) 33–40.
- [53] F.P. Zhao, E. Repo, Y. Meng, X.T. Wang, D.L. Yin, M. Sillanpää, An EDTA- β -cyclodextrin material for the adsorption of rare earth elements and its application in preconcentration of rare earth elements in seawater, *J. Colloid Interface Sci.*, 465 (2016) 215–224.
- [54] I. Liatsou, M. Efstathiou, I. Pashalidis, Adsorption of trivalent lanthanides by marine sediments, *J. Radioanal. Nucl. Chem.*, 304 (2015) 41–45.
- [55] A.A. Naser, G.E. Sharaf El-deen, A.A. Bhran, S.S. Metwally, A.M. El-Kamash, Elaboration of impregnated composite for sorption of europium and neodymium ions from aqueous solutions, *J. Ind. Eng. Chem.*, 32 (2015) 264–272.
- [56] A.A. Galhoum, M.G. Mafhouz, S.T. Abdel-Rehem, N.A. Gomaa, A.A. Atia, T. Vincent, E. Guibal, Cysteine-functionalized chitosan magnetic nano-based particles for the recovery of light and heavy rare earth metals: uptake kinetics and sorption isotherms, *Nanomaterials (Basel)*, 5 (2015) 154–179.
- [57] K. Li, Q. Gao, G. Yadavalli, X. Shen, H.W. Lei, B. Han, K.S. Xia, C.G. Zhou, Selective adsorption of Gd³⁺ on a magnetically retrievable imprinted chitosan/carbon nanotube composite with high capacity, *ACS Appl. Mater. Interfaces*, 7 (2015) 21047–21055.
- [58] D. Das, J.S. Varshini, N. Das, Recovery of lanthanum(III) from aqueous solution using biosorbents of plant and animal origin: batch and column studies, *Miner. Eng.*, 69 (2014) 40–56.
- [59] M.R. Awual, T. Kobayashi, H. Shiwaku, Y. Miyazaki, R. Motokawa, S. Suzuki, Y. Okamoto, T. Yaita, Evaluation of lanthanide sorption and their coordination mechanism by EXAFS measurement using novel hybrid adsorbent, *Chem. Eng. J.*, 225 (2013) 558–566.
- [60] Y. Liu, New insights into pseudo-second-order kinetic equation for adsorption, *Colloids Surf., A*, 320 (2008) 275–278.
- [61] H.N. Tran, S.-J. You, A. Hosseini-Bandegharai, H.-P. Chao, Mistakes and inconsistencies regarding adsorption of contaminants from aqueous solutions: a critical review, *Water Res.*, 120 (2017) 88–116.
- [62] S. Chakraborty, S. Chowdhury, P.D. Saha, Adsorption of crystal violet from aqueous solution onto NaOH-modified rice husk, *Carbohydr. Polym.*, 86 (2011) 1533–1541.

Supplementary information

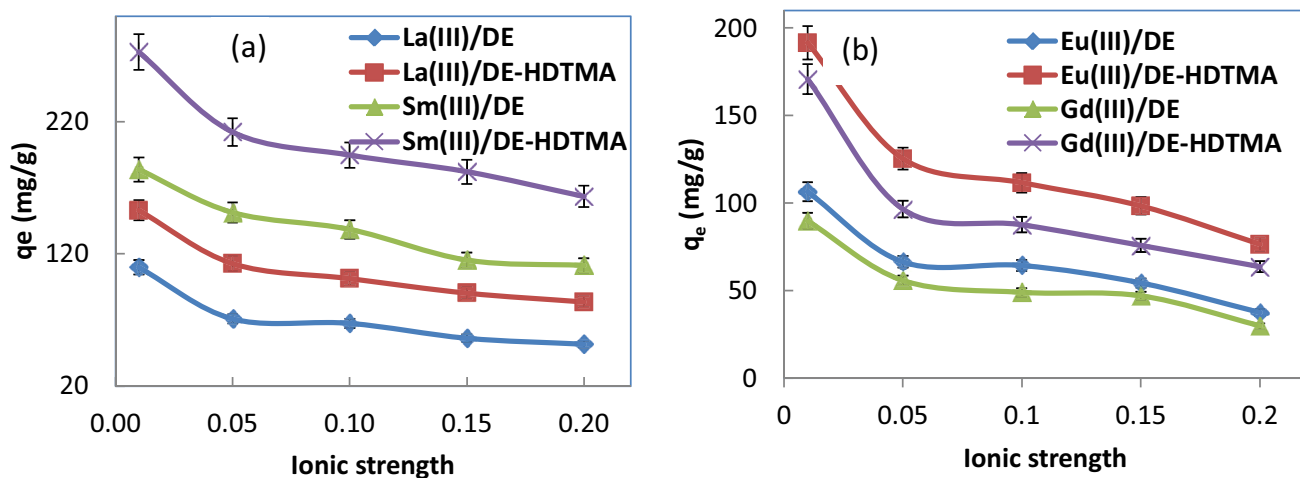


Fig. S1. Effect of ionic strength on the DE and DE-HDTMA adsorption efficiency for (a) La(III) and Sm(III) ions and (b) Eu(III) and Gd(III) ions. Initial metal ions concentration 30 mg L^{-1} ; pH = 5.0; adsorbent dosage 0.20 g/50 mL ; time of contact 24 h; temperature 25°C .

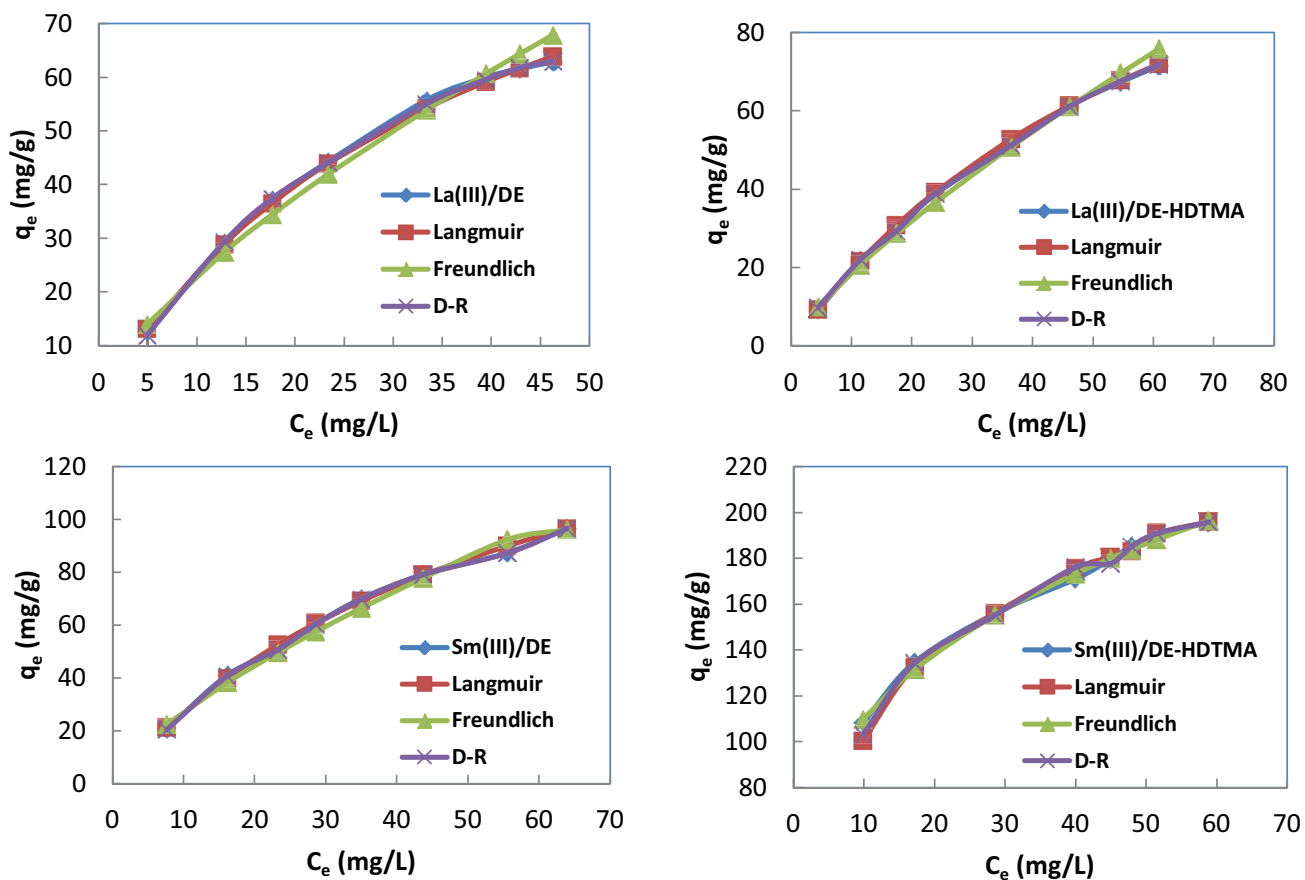


Fig. S2. Equilibrium isotherm for adsorption of La(III) and Sm(III) ions onto DE and DE-HDTMA, using the non-linear regression method. Initial metal ions concentration $10\text{--}50 \text{ mg L}^{-1}$; pH = 5.0; adsorbent dosage 0.20 g/50 mL ; temperature 25°C .

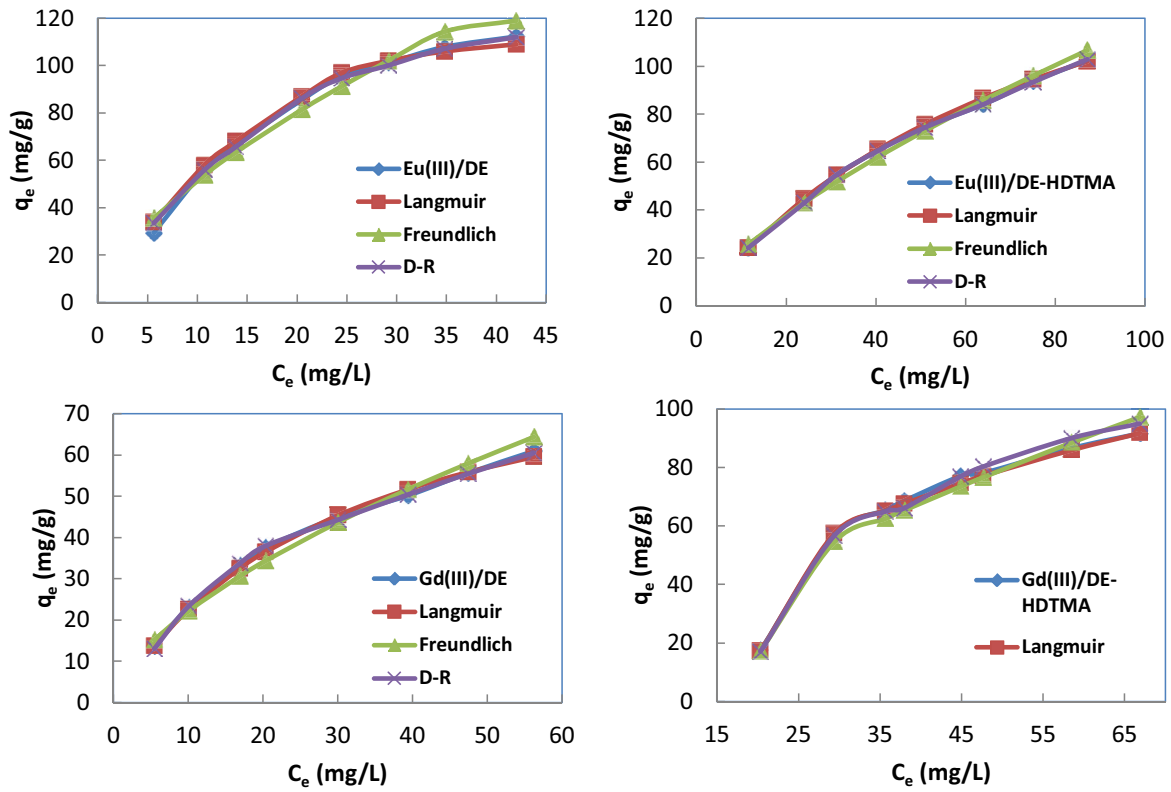


Fig. S3. Equilibrium isotherm for adsorption of Eu(III) and Gd(III) ions onto DE and DE-HDTMA, using the nonlinear regression method. Initial metal ions concentration 10–50 mg L⁻¹; pH = 5.0; adsorbent dosage 0.20 g/50 mL; temperature 25°C.

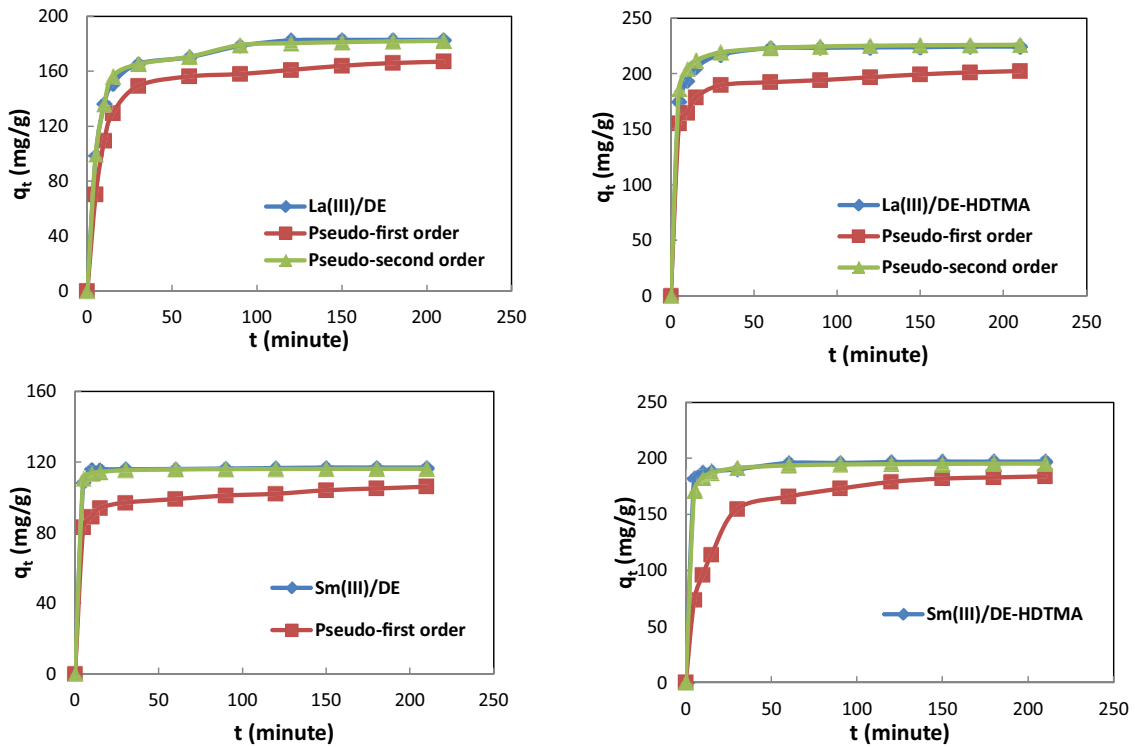


Fig. S4. Kinetic models for the adsorption of La(III) and Sm(III) ions onto DE and DE-HDTMA, using the non-linear regression method. Initial metal ions concentration 30 mg L⁻¹; pH = 5.0; adsorbent dosage 0.20 g/50 mL; temperature 25°C.

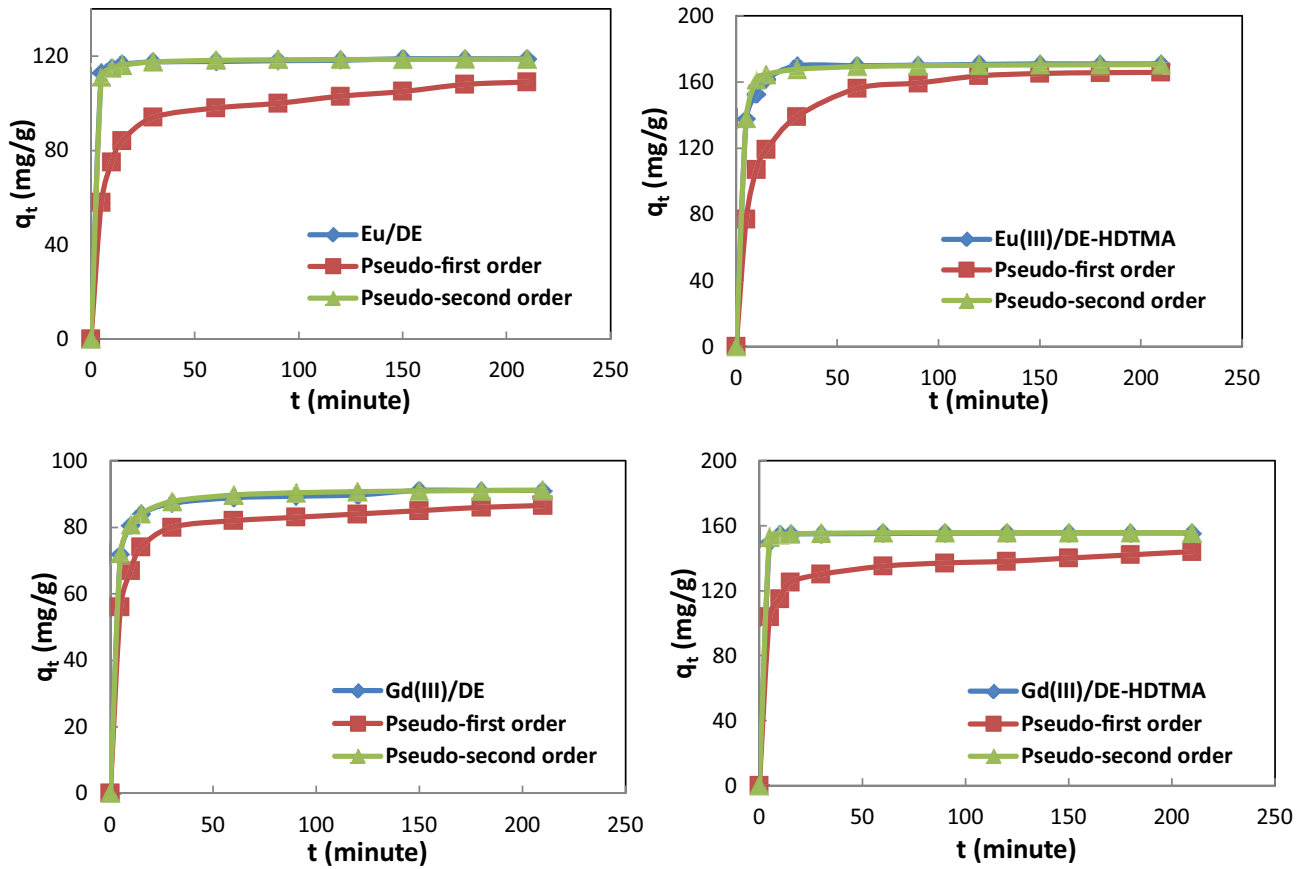


Fig. S5. Kinetic models for the adsorption of Eu(III) and Gd(III) ions onto DE and DE-HDTMA, using the non-linear regression method. Initial metal ions concentration 30 mg L^{-1} ; pH = 5.0; adsorbent dosage 0.20 g/50 mL ; temperature 25°C .

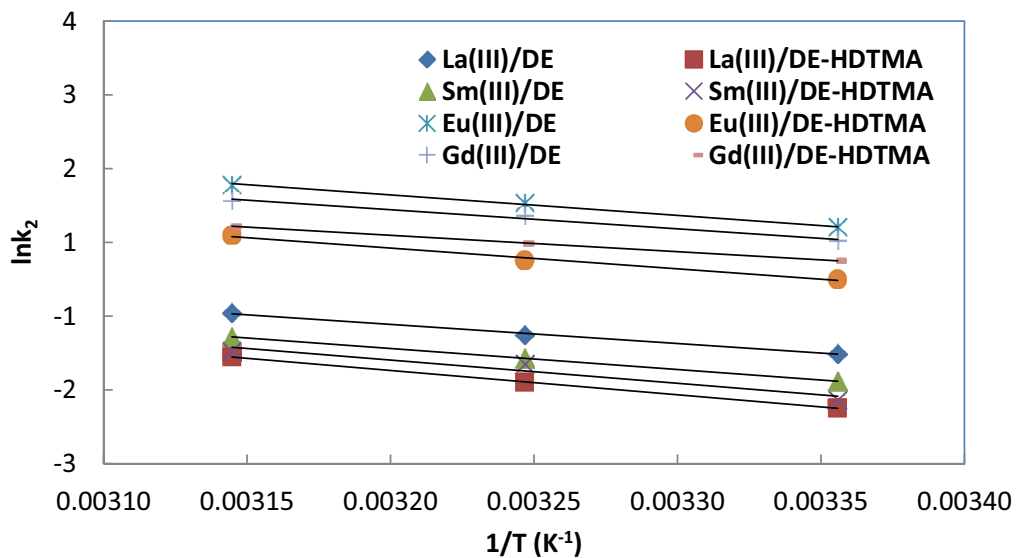


Fig. S6. Determination of E_a using the Arrhenius equation for the adsorption of La(III), Sm(III), Eu(III) and Gd(III) ions onto DE and DE-HDTMA.

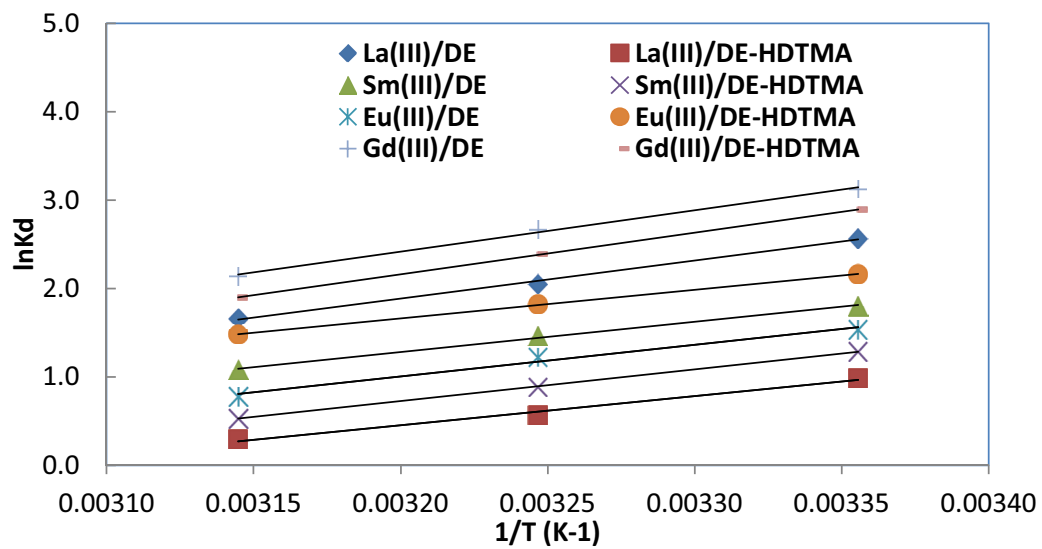


Fig. S7. Determination of ΔH° and ΔS° using the van't Hoff equation for the adsorption of La(III), Sm(III), Eu(III) and Gd(III) ions onto DE and DE-HDTMA.